

LA-UR- 08-6396

Approved for public release;
distribution is unlimited.

<i>Title:</i>	Direct photon production of d+A and A+A collisions at RHIC
<i>Author(s):</i>	Benwei Zhang, Ivan Vitev, T-2
<i>Intended for:</i>	European Journal of Physics C



Los Alamos National Laboratory, an affirmative action/equal opportunity employer, is operated by the Los Alamos National Security, LLC for the National Nuclear Security Administration of the U.S. Department of Energy under contract DE-AC52-06NA25396. By acceptance of this article, the publisher recognizes that the U.S. Government retains a nonexclusive, royalty-free license to publish or reproduce the published form of this contribution, or to allow others to do so, for U.S. Government purposes. Los Alamos National Laboratory requests that the publisher identify this article as work performed under the auspices of the U.S. Department of Energy. Los Alamos National Laboratory strongly supports academic freedom and a researcher's right to publish; as an institution, however, the Laboratory does not endorse the viewpoint of a publication or guarantee its technical correctness.

Direct photon production in d+A and A+A collisions at RHIC

Ben-Wei Zhang^{1,2} and Ivan Vitev¹

¹ Los Alamos National Laboratory, Theoretical Division, Mail Stop B283, Los Alamos, NM 87545, USA

² Institute of Particle Physics, Hua-Zhong Normal University, Wuhan 430079, China

Received: date / Revised version: date

Abstract. Direct photon productions in minimum bias d+Cu and d+Au and central Cu+Cu and Au+Au at center of mass energies $\sqrt{s} = 62.4$ GeV and 200GeV at RHIC are investigated systematically by taking into account jet quenching effect, medium-induced photon bremsstrahlung and jet-photon conversion in the hot QGP as well as known cold nuclear matter effects such as the isospin effect, the Cronin effect, shadowing effect, EMC effect and cold nuclear matter energy loss. It is shown that at high p_T the nuclear modification factor for direct photon $R_{AA}(p_T)$ is suppressed and dominated by cold nuclear matter effects, and there is no large enhancement due to medium-induced photon bremsstrahlung and jet-photon conversion in the hot QGP. Comparison of numerical simulations with experimental data rules out large Cronin enhancement and incoherent photon emission in medium, though large error bars in currently experimental data can not provide tight constraints on other nuclear matter effects.

PACS. 12.38.Mh – 24.85.+p – 12.38.Bx

1 Introduction

In relativistic heavy-ion collisions a large amount of energy is deposited in the colliding center when two nuclei colliding with each other at very high speed, and it is expected that quarks and gluons confined in nucleons may be liberated and a new kind of matter, quark-gluon plasma (QGP), should be formed. To tell whether this kind of matter is formed in heavy-ion collisions, many different QGP signatures have been proposed. From SPS to RHIC and to LHC, with higher and higher colliding energies, hard probes [1, 2], such as jet quenching, J/ψ suppression etc, become more and more important because of the asymptotic freedom of Quantum Chromodynamics (QCD): with larger momentum transfer, the running coupling constant becomes smaller and the perturbative calculations will be more reliable. The applications of hard probes with perturbative QCD (pQCD) are based on the factorization theorem, which separates the hard partonic part from the soft, non-perturbative part. For a physics observable $dF/d^2\mathbf{p}_T$ in p+p collisions, the factorization theorem of pQCD tells that

$$\frac{dF}{d^2\mathbf{p}_T} \propto \phi_{a/A}(\xi_A, \mu_f) \phi_{b/B}(\xi_B, \mu_f) \times \frac{d\hat{F}^{a+b \rightarrow c+X}}{d^2\mathbf{p}_T} \otimes D_{h/c}(z, \mu_f). \quad (1)$$

Here $d\hat{F}^{a+b \rightarrow c+X}/d^2\mathbf{p}_T$ represents the correspondent partonic contribution, while $\phi_{a/A}(\xi_A, \mu_f)$ and $D_{h/c}(z, \mu_f)$ are the parton distribution function (PDF) and parton fragmentation function (PFF) respectively, which stand for

the non-perturbative parts. In nucleus-nucleus collisions, if the QGP is created, final-state interaction in the hot/dense medium may modify parton fragmentation functions effectively and change the value of $dF/d^2\mathbf{p}_T$. However, as shown in Eq. (1) the initial-state cold nuclear effects will modify the parton distribution function, and thus alter $dF/d^2\mathbf{p}_T$ in A+A collisions, too. Therefore, A robust calculation for hard probes as QGP signatures need better control of the initial-state cold nuclear effects.

Because the photon interacts with the partons in the collisional region only through electromagnetic interaction ($\alpha_{EM} \ll \alpha_s$) and its mean free path is quite large, the produced photon may leave the medium without rescattering and its production can provide a promising observable to constrain the initial-state cold nuclear effects. The study of photon production is also interesting in its own right because recently two novel mechanisms of photon production in the QGP have been proposed: medium-induced photon emission in the QGP [3] and jet-photon conversion in the QGP [4], which are argued to give large enhancement of direct photon production in central heavy-ion collisions. To see the magnitudes of these enhancement and obtain better constraints on initial-state nuclear effects, a systematic study of direct photon production in different nuclear systems with different center of mass energies by including all relevant cold nuclear effects (isospin effect, Cronin effect, shadowing effect, cold nuclear matter energy loss, EMC effect) and hot nuclear medium effects (jet quenching, medium-induced photon bremsstrahlung, jet-photon conversion) will be indispensable [5]. We will focus on direct photon productions at large transverse momentum

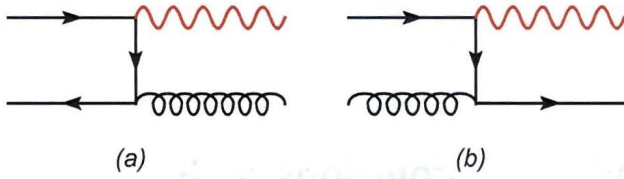


Fig. 1. Direct photon production from the annihilation process (Diagram (a)) and the Compton process (Diagram (b)) .

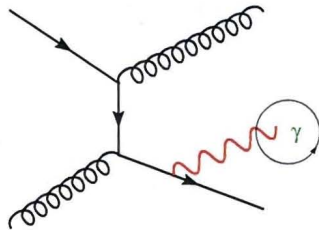


Fig. 2. Direct photon production from the bremsstrahlung (fragmentation) process.

in minimum bias d+Cu and d+Au and central Cu+Cu and Au+Au heavy ion collisions at RHIC with center of mass energies $\sqrt{s} = 62.4$ GeV and 200 GeV by taking into account all involved hot and cold nuclear matter effects.

2 Direct photon production in p+p collisions

In 'elementary' p+p collisions, direct photon can be produced by the annihilation process ($q + \bar{q} \rightarrow \gamma g$) and the Compton process ($q + g \rightarrow \gamma q$) at leading-order in perturbative theory, as shown in Fig. 1. Also we should include the contribution of bremsstrahlung process illustrated in Fig. 2. At first glance, it seems that bremsstrahlung process gives higher-order contribution ($\alpha\alpha_s^2$) as compared to the annihilation and the Compton processes ($\alpha\alpha_s$). However, noticing in bremsstrahlung process there is a photon fragmentation function $D_{\gamma/c}(z, Q^2)$, which absorbs the collinear singularity and has a logarithmic growth with the hard scale Q^2 [6], we have

$$\begin{aligned} \alpha_s(Q) &\propto \ln^{-1}\left(\frac{Q^2}{\Lambda^2}\right), \quad D_{\gamma/c}(z, Q^2) \propto \ln\left(\frac{Q^2}{\Lambda^2}\right) \\ \alpha\alpha_s^2(Q^2)D_{\gamma/c}(z, Q^2) &\propto \alpha\alpha_s(Q^2). \end{aligned} \quad (2)$$

Hence the contribution of bremsstrahlung process is effectively the same order as those of the annihilation process and the Compton process, and should be taken into account even in leading-order calculations.

In our leading-order pQCD model, the cross section of direct photon production in p+p collision is given:

$$\begin{aligned} \frac{d\sigma_{pp}^{\gamma}}{dy d^2\mathbf{p}_T} &= K \sum_{abcd} \int dy_a \int d^2\mathbf{k}_a d^2\mathbf{k}_b \frac{f(k_b)f(k_b)}{|J(k_a, k_b)|} \\ &\times \frac{\phi_{a/N}(x_a, \mu_f)\phi_{b/N}(x_b, \mu_f)}{x_a x_b} \end{aligned}$$

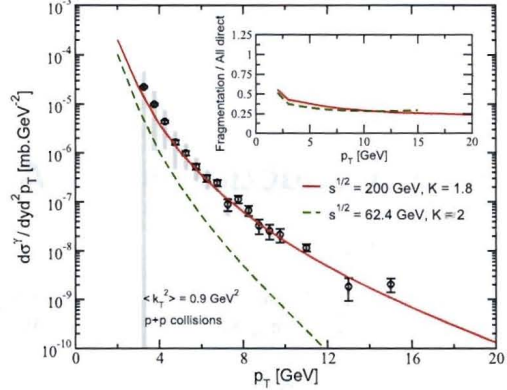


Fig. 3. Cross sections of direct γ production in p+p collisions at $\sqrt{s} = 62.4$ GeV and 200 GeV. Data at $\sqrt{s} = 200$ GeV is taken from PHENIX [7]. Insert gives the ratio of bremsstrahlung photons to all direct photons.

$$\times \int \frac{dz}{z^2} D_{\gamma/c}(z, \mu_{fr}) \frac{\alpha_s(\mu_r)\alpha_c}{2S} |\overline{M}|^2, \quad (3)$$

and the detail of the notations used in above formula can be seen in [5, 10, 17]. Here we emphasize that though we use a phenomenological K-factor to take into account next-to-leading order calculations, this K-factor will cancel when we calculate the nuclear modification factor $R_{AB}(p_T)$. In Fig. 3 we show our numerical results of the cross sections for direct photon in p+p collisions at $\sqrt{s} = 62.4$ GeV and $\sqrt{s} = 200$ GeV. It could be seen that our model can describe quite well the data of direct photon in p+p at 200 GeV measured by PHENIX [7]. The insert in Fig. 3 gives the fraction of bremsstrahlung (fragmentation) photons to all direct photons. It could be seen that at very high p_T , bremsstrahlung photons contribution about $\sim 25\% - 30\%$ of total direct photons in p+p collisions.

3 Direct photon production in heavy-ion collisions: hot nuclear matter effects

In ultra-relativistic central nucleus-nucleus collisions, when a hot QGP is formed, this new kind of hot nuclear matter will affect direct photon production by different jet-medium interactions.

3.1 Jet quenching in the QGP

It is well known that when an energetic parton propagating in the hot/dense nuclear medium, it may suffer multiple scattering and lose a large amount of energy via induced gluon radiation [1, 8, 9]. This jet quenching effect may reduce the contribution of bremsstrahlung (fragmentation) photons since before a jet fragmenting into photon, it may lose energy due to passing through the hot medium. We calculate the energy loss of the jet within

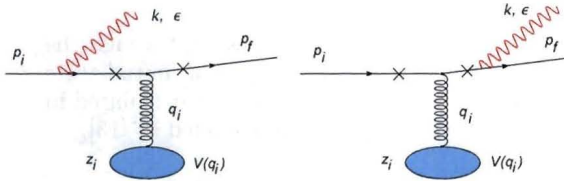


Fig. 4. Single-Born diagrams for medium-induced γ emission

GLV formalism [8], where the fragmentation functions for photon in medium could be given effectively as

$$D_{\gamma/c}(z) \Rightarrow \int_0^{1-z} d\epsilon P(\epsilon) \frac{1}{1-\epsilon} D_{\gamma/c} \left(\frac{z}{1-\epsilon} \right) . \quad (4)$$

Here, $P(\epsilon)$ is the probability distribution of the fractional jet energy loss $\epsilon = \Delta E/E$ [10].

3.2 Medium-induced photon radiation

In the hot QGP, a propagating jet may also radiate an induced photon due to multiple scattering in the medium [3, 11, 12]. Because there is no gauge-boson self-interactions in photon bremsstrahlung, one may expect that photon emission in medium is a simple degeneration of medium-induced gluon emission. However carefully investigation shows that this naive expectation is not true. Considering the radiative amplitude for single scattering of a fast on-shell quark [8]:

$$\mathcal{M}_{rad}(k) \propto 2ig_s \epsilon_{\perp} \cdot \left(\frac{\mathbf{k}_{\perp}}{\mathbf{k}_{\perp}^2} - \frac{(\mathbf{k} - \mathbf{q})_{\perp}}{(\mathbf{k} - \mathbf{q})_{\perp}^2} \right) e^{i\frac{\mathbf{k}^2}{2k} z^+} [T^c, T^a] , \quad (5)$$

if we take QED limit that $T^{a,c} \rightarrow 1$, we obtain $\mathcal{M}_{rad}^{\gamma}(k) \rightarrow 0$. Thus Therefore, a theoretical approach developed to describe medium induced gluon radiation cannot be directly generalized to photon bremsstrahlung in medium and vice versa [5, 11].

Here we derive the contribution of medium-induced photon emission with the Reaction Operator Expansion approach developed by GLV [8]. For the single-Born scattering diagrams illustrated in Fig. 5, we get [5]

$$\mathcal{M}_{rad}(k, \{i\}) = e \left(\frac{\epsilon \cdot p_f}{k \cdot p_f} - \frac{\epsilon \cdot p_i}{k \cdot p_i} \right) e^{iz_i^+ k^-} , \quad (6)$$

where the collisional amplitude is not shown. The contribution of Double-Born diagrams, which give the virtual corrections, is found to be negligible as

$$\mathcal{M}_{rad}^V(k) \approx 0 . \quad (7)$$

Extending the above calculations to higher orders of opacity expansion, we demonstrate that contributions of medium-induced photon emission vanish beyond second order in opacity, and the final results can be given as [5],

$$\mathcal{M}_{rad}^V(k) \approx 0$$

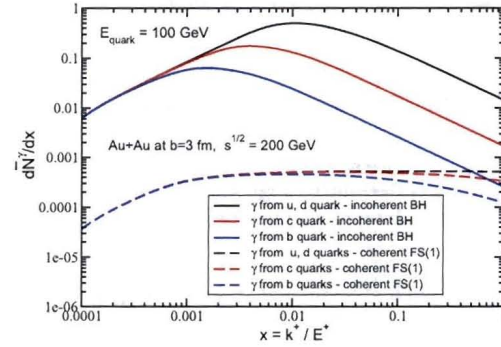


Fig. 5. Scaled medium-induced photon number spectrum versus $x = k^+/E^+$ for $E_q = 100$ GeV light, charm and bottom quarks in central Au+Au collisions at $\sqrt{s} = 200$ GeV, where solid curves stand for the incoherent photon radiation in medium, and dash curves for the coherent photon bremsstrahlung.

$$k^+ \frac{dN^{\gamma}(k)}{dk^+ d^2\mathbf{k}_{\perp}} = \frac{\alpha_{em}}{\pi^2} \left\{ \int \frac{d\Delta z_1}{\lambda_q(z_1)} \int d^2\mathbf{q}_{\perp 1} \frac{1}{\sigma^{\text{el}}} \frac{d^2\sigma^{\text{el}}}{d^2\mathbf{q}_{\perp 1}} \right. \\ \times [|\mathcal{M}_{rad}(\{1\})|^2 + 2\mathcal{M}_{rad}^*(\{1\})\mathcal{M}_{rad}(\{0\}) \cos(k^- \Delta z_1^+)] \\ + \text{correction} . \quad (8)$$

Here $\Delta z_i^+ = z_i^+ - z_{i-1}^+$, and $\tau_f^{-1} = \mathbf{k}^2/(2\omega) \approx \sqrt{2} k^-$ is the inverse photon formation time. There are two limits in Eq. (8): when $\tau_f^{-1} \lambda_q \gg 1$, the contribution from $\cos(k^- \Delta z_i^+)$ will vanish due to large oscillation and we will reach to incoherent limit; otherwise the interference term will not vanish and we go to coherent photon radiation region. Also we find in heavy-ion collisions the number of interactions $\langle n \rangle = L/\lambda_q = 2-3$. These properties are different from those in previous studies [3, 12]. In Fig. 5 we show the numerical results of scaled medium-induced photon number spectrum $d\bar{N}^{\gamma}/dx = (e/e_q)^2 dN^{\gamma}/dx$, $x = k^+/E^+$ for a quark jet propagating outwards from the center of the medium created in $b = 3$ fm Au+Au collisions at RHIC. It could be seen that interference effect will greatly suppress the coherent photon radiation in medium as compared to the incoherent photon radiation.

3.3 Jet-photon conversion

In the hot/dense medium, another interesting source of direct photon production is the jet-photon conversion [4], where a quark jet may be converted into a high energy photon via the process illustrated in Fig. 6 when passing through a gluon-dominated QGP. Taking the approximation that $p_{\gamma} \approx p_c$ in the forward scattering process, we can derive the jet-photon probability as,

$$N_{\text{conv.}}^{\gamma}(c) = \int_{t_0}^L dt \rho(T) \sigma_{\text{tot}}^{qg \rightarrow \gamma q}(T) , \quad (9)$$

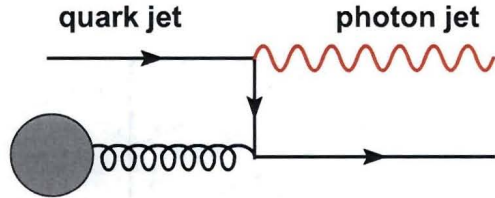


Fig. 6. A quark jet is converted into a high energy photon via interacting with a thermal gluon in the hot QGP.

where the cross section with $s \approx 2m_D E$ and $t \in (m_D^2, s/4)$, is given by

$$\sigma^{qg \rightarrow \gamma q} = \frac{\pi \alpha_s \alpha_{em}}{6m_D E} \ln \frac{E}{2m_D} . \quad (10)$$

3.4 total contributions to direct photon

Combining the above discussions, we can incorporate the total contributions to direct γ productions due to different kinds of the final-state jet-medium interactions in the QGP by:

$$D_{\gamma/c}(z) \Rightarrow \int_0^{1-z} d\epsilon P(\epsilon) \frac{1}{1-\epsilon} D_{\gamma/c} \left(\frac{z}{1-\epsilon} \right) + \frac{dN_{\text{med.}}^{\gamma}(c)}{dz} + N_{\text{conv.}}^{\gamma}(c) \delta(1-z) , \quad (11)$$

where the first term takes into account jet quenching effect to fragmentation photon production, the second term gives addition contribution to photon production from medium-induced photon, the last one stands for contribution from jet-photon conversion.

4 Direct photon production in heavy-ion collisions: cold nuclear matter effects

Even though in p+A collisions there are no final-state hot nuclear medium effects, A p+A collision still can not be regarded as a simple superposition of p+p collisions. There are many cold nuclear matter effects in p+A collisions, which of course will manifest themselves in A+A collisions, and thus alter the cross section of direct photon production in p+A collisions and A+A collisions.

4.1 Isospin effect

The cross sections of direct photon production for p+p, p+n and n+n collisions are different because these cross sections depend on the electric charges of quarks ($\sigma \propto \sum_q e_q^2$), and in constituent quark model $p = |uud\rangle$ and $n = |udd\rangle$, while u quark and d quark have different electric charges. We will show later that this isospin effect may impose significant impact on the nuclear modification factor of direct photon production $R_{AB}(p_T)$.

4.2 Initial-state energy loss in cold nuclei

Before hard scattering a fast parton passing through the cold nuclear matter may also lose energy. This initial-state energy loss in cold nuclear matter has been calculated in GLV formalism and the effect can be modeled as [13],

$$\begin{aligned} \phi_{a,b/N}(x_{a,b}, Q^2) &\rightarrow \phi_{a,b/N} \left(\frac{x_{a,b}}{1 - \epsilon_{a,b}}, Q^2 \right) \\ &\approx \phi_{a,b/N} (x_{a,b}(1 + \epsilon_{a,b}), Q^2) \end{aligned} \quad (12)$$

where $\epsilon_{a,b}$ are the fractional energy losses for the incoming partons a, b evaluated in the rest frame of the corresponding target nucleus with $\epsilon_{a,b} \ll 1$. In numerical calculation the effect of multi-gluon fluctuation has been taken into account [5, 14].

4.3 Cronin effect

The initial-state multiple scattering in cold nuclear matter will broaden the transverse momenta of incoming partons before hard scattering. In our calculation, the k_T broadening due to the Cronin effect is given as [15, 16],

$$\begin{aligned} \langle k_T^2 \rangle &= \langle k_T^2 \rangle_{pp} + \langle k_T^2 \rangle_{med} , \\ \langle k_T^2 \rangle_{med} &= \left(\frac{2\mu^2 L}{\lambda} \right)_{q,g} \times \max[1, \ln(1 + \delta p_T^2)] \end{aligned} \quad (13)$$

with $\mu^2 = 0.12 \text{ GeV}^2$, $\lambda_g = (C_F/C_A)\lambda_q = 1 \text{ fm}$ and $\delta = 0.3$ fixed by fitting p+A data.

4.4 Shadowing effect

In our model, the shadowing effect was calculated from the coherent final-state parton interactions within higher-twist collinear factorization approach in pQCD [17], and the scale of power correction power ξ^2 is the only parameter constrained by the mean squared momentum transfer per unit length μ^2/λ as $(\xi^2 A^{1/3})_{q,g} \approx (2\mu^2 L/\lambda)_{q,g}$ in minimum bias collisions.

4.5 EMC effect

In this investigation, we incorporate the EMC effect by using EKS parametrization [18]. In our numerical results shown in Sect. 5 it is shown that the contribution from EMC effect is rather small.

5 Numerical results

With the leading-order pQCD improved parton model in Eq. (3) by including all hot QGP medium effects calculated in Sect. 3 and cold nuclear matter effects discussed

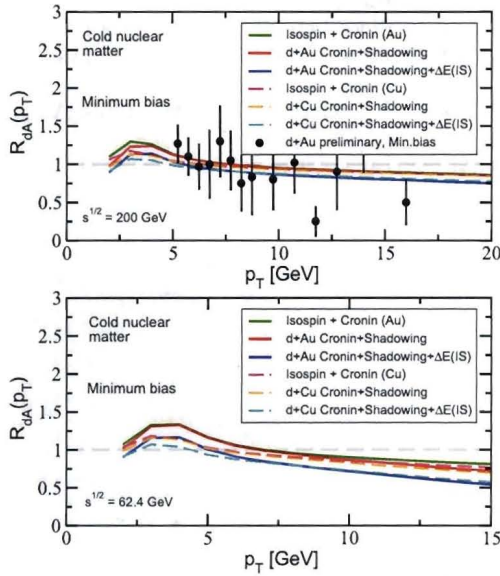


Fig. 7. Nuclear modification factors for direct photon $R_{dAu}(p_T)$ in minimum bias d+Au (solid lines) and d+Cu (dashed lines) collisions at $\sqrt{s} = 62.4$ GeV (bottom panel) and 200 GeV (top panel) with preliminary $\sqrt{s} = 200$ GeV minimum bias d+Au data from PHENIX [10].

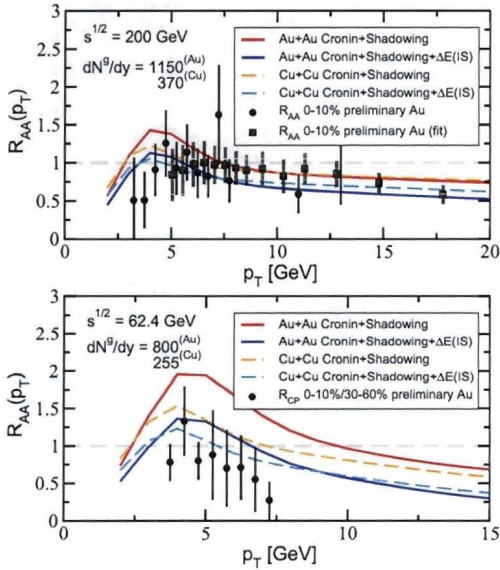


Fig. 8. $R_{AA}(p_T)$ for direct photon in central Au+Au and Cu+Cu collisions at $\sqrt{s} = 62.4$ GeV (bottom panel) and $\sqrt{s} = 200$ GeV (top panel) by including all cold nuclear effects and jet quenching effect of bremsstrahlung photons and relevant data are taken from [7, 20].

in Sect. 4, we can calculate numerically the nuclear modification factors

$$R_{AB}(p_T, b) = \frac{d\sigma_{AB}}{dy d^2 \mathbf{p}_T} \Big/ N_{AB}^{\text{coll}}(b) \frac{d\sigma_{pp}}{dy d^2 \mathbf{p}_T},$$

and compare them with available experimental data at RHIC. Since we focus on hard photon production, the contribution from thermal photon will be very small and will be neglected in current study.

Fig. 7 shows the numerical results for minimum-bias d+Au and d+Cu collisions at different colliding energies $\sqrt{s} = 62.4, 200$ GeV. We observe that when $p_T < 6$ GeV, the Cronin effect is dominant and gives an enhancement, while $p_T > 6$ GeV, the isospin effect becomes the most important, which suppress $R_{dA}(p_T)$ considerably with substantial contribution from the initial-state energy loss effect. It is interesting to note that the cold nuclear effects have reduced direct photon production at $p_T \sim 15$ GeV by about 25% for d+A collisions at $\sqrt{s} = 200$ GeV, and by about 40% for those at $\sqrt{s} = 200$ GeV. The cold nuclear effects are more pronounced in d+A collisions at $\sqrt{s} = 62.4$ GeV because the direct photon spectrum in p+p collisions at $\sqrt{s} = 62.4$ GeV is steeper than that at $\sqrt{s} = 200$ GeV as shown in Fig. 3. Due to big error bars in data, the current experimental measurements in d+A could not tightly constrain the different cold nuclear effects.

We show the results in central Au+Au and Cu+Cu collisions with $\sqrt{s} = 62.4$ GeV and 200 GeV in Fig. 8. Fig. 9, with the former focus on cold nuclear effects. By comparing Fig. 8 with Fig. 7 one can see that in A+A collisions $R_{AA}(p_T)$ for direct photon production is dominated by cold nuclear effects, and amplified by the existence of two large nuclei. The experimental data have excluded large Cronin enhancement. From Fig. 9 one can see the incoherent medium-induced photon emission is ruled out by the experimental data. It is found that Jet conversion contributes $\sim 25\%$ at $p_T < 5$ GeV, and contribution from medium-induced photon is about 10%. At high p_T region, the two enhancement contributions are rather small and $R_{AA}(p_T)$ is significant suppressed. With our systematic study we did not see large enhancement of direct photon production due to medium-induced photon emission and jet-photon conversion in the hot QGP.

6 Conclusions

By taking into relevant cold nuclear effects and the hot QGP medium effects we carry out a systematic study of direct photon production in p+A and A+A collisions at RHIC. It is demonstrated that by comparing theoretical calculations with available experimental measurements of direct photon, the large Cronin enhancement and incoherent medium-induced photon bremsstrahlung are contradicted with experimental data, though large error bars in data could not provide further constraints on the magnitudes of different nuclear effects. Also it is shown that though medium-induced photon and jet-photon conversion will enhance direct photon at intermediate p_T in A+A

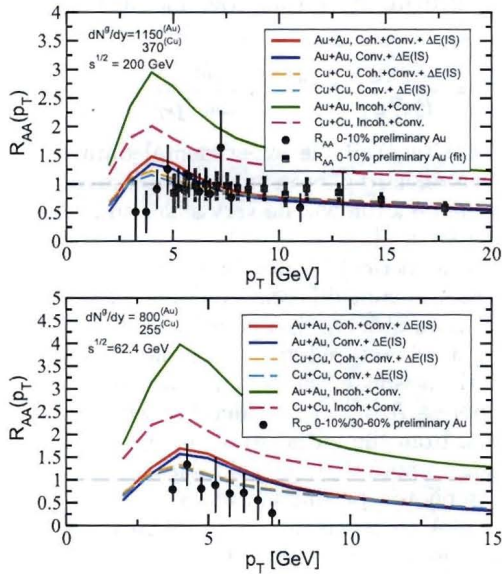


Fig. 9. The same as in Fig. 8 except that in this figure all cold nuclear effects and hot QGP medium effects are included.

collisions, large enhancement due to these two direct photon production mechanism in the hot QGP is absent.

Acknowledgments: This research is supported by the US Department of Energy, Office of Science, under Contract No. DE-AC52-06NA25396 and in part by the LDRD program at LANL, the NNSF of China and the MOE of China under Project No. IRT0624.

References

1. M. Gyulassy, I. Vitev, X. N. Wang and B. W. Zhang, arXiv:nucl-th/0302077.
2. A. Accardi *et al.*, arXiv:hep-ph/0310274.
3. B. G. Zakharov, JETP Lett. **80**, 1 (2004) [Pisma Zh. Eksp. Teor. Fiz. **80**, 3 (2004)].
4. R. J. Fries, B. Muller and D. K. Srivastava, Phys. Rev. Lett. **90** (2003) 132301 [arXiv:nucl-th/0208001].
5. I. Vitev and B. W. Zhang, arXiv:0804.3805 [hep-ph].
6. J. F. Owens, Rev. Mod. Phys. **59**, 465 (1987).
7. S. S. Adler *et al.* [PHENIX Collaboration], Phys. Rev. Lett. **98**, (2007) 012002.
8. M. Gyulassy, P. Levai and I. Vitev, Nucl. Phys. B **594**, 371 (2001).
9. X. N. Wang and X. F. Guo, Nucl. Phys. A **696**, 788 (2001); B. W. Zhang and X. N. Wang, Nucl. Phys. A **720**, 429 (2003).
10. I. Vitev, Phys. Lett. B **639**, 38 (2006).
11. B. W. Zhang and E. K. Wang, Chin. Phys. Lett. **20** (2003) 639.
12. P. Arnold, G. D. Moore and L. G. Yaffe, JHEP **0112**, 009 (2001); JHEP **0111**, 057 (2001).
13. I. Vitev, Phys. Rev. C **75**, 064906 (2007).
14. M. Gyulassy, P. Levai and I. Vitev, Phys. Lett. B **538**, 282 (2002).
15. I. Vitev and M. Gyulassy, Phys. Rev. Lett. **89**, 252301 (2002).
16. I. Vitev, Phys. Lett. B **562**, 36 (2003).
17. J. W. Qiu and I. Vitev, Phys. Lett. B **632**, 507 (2006).
18. K. J. Eskola, V. J. Kolhinen and C. A. Salgado, Eur. Phys. J. C **9** (1999) 61.
19. D. Peressounko [PHENIX Collaboration], Nucl. Phys. A **783**, 577 (2007).
20. T. Sakaguchi, arXiv:0805.4644 [nucl-ex].